

# Semileptonic $B$ decays into even parity charmed mesons

M. De Vito<sup>1,2</sup>, P. Santorelli<sup>1,2,a</sup>

<sup>1</sup> Dipartimento di Scienze Fisiche, Università di Napoli “Federico II”, Italy

<sup>2</sup> Istituto Nazionale di Fisica Nucleare, Sezione di Napoli, Italy

Received: 1 August 2006 /

Published online: 24 October 2006 – © Springer-Verlag / Società Italiana di Fisica 2006

**Abstract.** By using a constituent quark model we compute the form factors relevant to semileptonic transitions of the  $B$  mesons into low-lying  $p$ -wave charmed mesons. We evaluate the  $q^2$  dependence of these form factors and compare them with other model calculations. The Isgur–Wise functions  $\tau_{1/2}$  and  $\tau_{3/2}$  are also obtained in the heavy quark limit of our results.

**PACS.** 13.25.Hw; 12.39.Hg; 12.39.Jh

## 1 Introduction

Recently, the BaBar Collaboration has discovered a narrow state with  $J^P = 0^+$  with a mass of 2317 MeV,  $D_{s0}^*(2317)$ . The existence of a second narrow resonance,  $D_{sJ}(2460)$  with  $J^P = 1^+$ , was confirmed by CLEO [2]. Both states have been confirmed by BELLE [3]. Soon after the discovery, another set of charmed mesons,  $D_0^{*0}(2308)$  and  $D_1^{*0}(2427)$ , which have the same quantum numbers,  $J^P = (0^+, 1^+)$ , as  $D_{sJ}$ , has been discovered by BELLE [4]. Before their discovery, quark model and lattice calculations predicted that the masses of these states, in particular  $D_{s0}^*(2317)$  and  $D_{s1}'(2460)$ , would be significantly higher than observed [5–9]. Moreover, these states were predicted to be broad due to the fact that they can decay into  $DK$  and  $D^*K$ , respectively. Experimentally, the masses of  $D_{s0}^*(2317)$  and  $D_{s1}'(2460)$  are below the  $DK$  and  $D^*K$  thresholds and hence they are very narrow. These facts inspired a lot of theorists to explain the puzzle [10].

In this paper we will focus our attention on the weak semileptonic transitions of  $B$  mesons into lower-lying  $p$ -wave charmed mesons ( $D^{**}$ ). These transitions were studied, within a quark model approach, for the first time in [11, 12] and, more recently, in [13–19] where the authors take into account the symmetries of QCD for heavy quarks [20–23], already used in [24]. The light-front covariant model [25] was adopted to study the same subject in [26]. The relevant form factors were also evaluated, in the framework of QCD sum rules [27–29], in [30–34].

Here we employ a simple constituent quark model [35–37] to evaluate the semileptonic form factors of the  $B$  mesons into  $p$ -wave charmed mesons. The plan of

the paper is the following. In the next section we describe our quark model; the third section is devoted to the introduction and evaluation of the  $s$ -wave to  $p$ -wave form factors. Our way to fix the free parameters of the model and the resulting form factors are discussed in Sect. 4, while in section five the heavy quark limit of the form factors are computed and compared with heavy quark effective theory predictions; the  $\tau_{1/2}$ , and  $\tau_{3/2}$  are also evaluated. In the last section we show and discuss our numerical results.

## 2 A constituent quark model

In our model [35–37] any heavy meson  $H(Q\bar{q})$ , with  $Q \in \{b, c\}$  and  $q \in \{u, d, s\}$ , is described by the matrix

$$H = \frac{1}{\sqrt{3}} \psi_H(k) \frac{q_1 + m_Q}{2m_Q} \Gamma \frac{-q_2 + m_q}{2m_q}, \quad (1)$$

where  $m_Q$  ( $m_q$ ) stands for the heavy (light) quark mass;  $q_1^\mu, q_2^\mu$  are their 4-momenta (cf. Fig. 1).  $\psi_H(k)$  indicates the meson’s wave function which is fixed by using a phenomenological approach. The meson-constituent quarks vertexes,  $\Gamma$  in (1), are fixed by using the correct transformation properties under  $C$  and  $P$ , and to enforce the relation

$$\begin{aligned} \langle H | H \rangle &\equiv \text{Tr}\{(-\gamma_0 H^\dagger \gamma_0) H\} \\ &= \int \frac{d^3 k}{(2\pi)^3} |\psi_H(k)|^2 = 2M_H. \end{aligned} \quad (2)$$

For the odd parity,  $s$ -wave heavy mesons  $J^P = (0^-, 1^-)$ , and  $\Gamma$  is given by

<sup>a</sup> e-mail: pietro.santorelli@na.infn.it

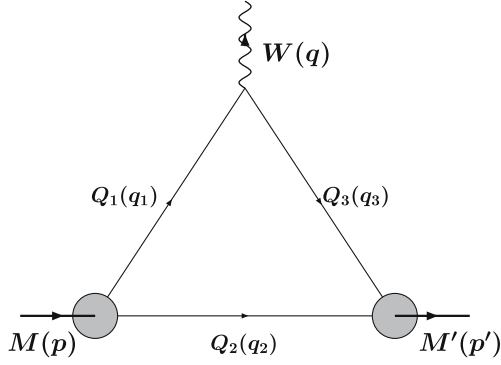


**Fig. 1.** Quark model diagram for the hadronic amplitude relevant to semileptonic  $M \rightarrow M'$  decay involving  $Q_1 \rightarrow Q_3$  transitions. The thin lines represent quarks, the thick ones mesons. The gray disks represent the quark-quark-meson vertexes

$$\Gamma_{0-} = -i\gamma_5 \sqrt{\frac{2m_Q m_q}{m_H^2 - (m_Q - m_q)^2}}, \quad (3)$$

$$\begin{aligned} \Gamma_{1-}(\varepsilon, q_1, q_2) &= \varepsilon_\mu \left[ \gamma^\mu - \frac{q_1^\mu - q_2^\mu}{m_H + m_Q + m_q} \right] \\ &\times \sqrt{\frac{2m_Q m_q}{m_H^2 - (m_Q - m_q)^2}}, \end{aligned} \quad (4)$$

where  $\varepsilon$  is the polarization 4-vector of the (vector) meson  $H$ . The vertexes of the lower-lying even parity heavy mesons, instead, are given by the matrices<sup>1</sup>

$$\Gamma^{3P_0} = \Gamma_{0+} = -i\sqrt{\frac{2m_Q m_q}{m_H^2 - (m_Q + m_q)^2}}, \quad (5)$$

$$\begin{aligned} \Gamma^{3P_1}(\varepsilon, q_1, q_2) &= \varepsilon_\mu \left[ \gamma^\mu - \frac{(m_Q - m_q)(q_1^\mu - q_2^\mu)}{-m_H^2 + (m_Q - m_q)^2} \right] \\ &\times \gamma_5 \sqrt{\frac{3m_Q m_q}{m_H^2 - (m_Q + m_q)^2}}, \end{aligned} \quad (6)$$

$$\begin{aligned} \Gamma^{1P_1}(\varepsilon, q_1, q_2) &= \varepsilon_\mu \left[ \frac{(q_1^\mu - q_2^\mu)m_H}{m_H^2 - (m_Q - m_q)^2} \right] \\ &\times \gamma_5 \sqrt{\frac{6m_Q m_q}{m_H^2 - (m_Q + m_q)^2}}. \end{aligned} \quad (7)$$

As already discussed in [35–37], the 4-momentum conservation in the meson-constituent quarks vertexes can be obtained defining a heavy running quark mass. For details we refer the reader to [35–37]. Here, for the sake of utility, we recall all the remaining rules of our model for the evaluation of the hadronic matrix elements of weak currents:

a) for each quark loop with 4-momentum  $k$  we have

$$\int \frac{d^3 k}{(2\pi)^3}, \quad (8)$$

a colour factor of 3 and a trace over the Dirac matrices;

b) for the weak hadronic current,  $\bar{q}_2 \Gamma^\mu q_1$ , one puts the factor

$$\sqrt{\frac{m_1}{E_1}} \sqrt{\frac{m_2}{E_2}} \Gamma^\mu, \quad (9)$$

where with  $\Gamma^\mu$  we indicate a combination of Dirac matrices.

### 3 Form factors

In this section we evaluate the form factors parameterizing the  $0^- \rightarrow (0^-, 1^-)$  and  $0^- \rightarrow (0^+, {}^3P_1, {}^1P_1)$  weak transitions. The decomposition of these matrix elements of weak currents in terms of form factors are the following (see also [11, 12]):

$$\begin{aligned} \langle H'_{0-}(p') | V_\mu | H_{0-}(p) \rangle \\ = f_+(q^2) (p_\mu + p'_\mu) + f_-(q^2) (p_\mu - p'_\mu), \end{aligned} \quad (10)$$

$$\begin{aligned} \langle H'_{1-}(p', \varepsilon) | V_\mu - A_\mu | H_{0-}(p) \rangle \\ = 2g(q^2) \epsilon^{\mu\nu\alpha\beta} \varepsilon_\nu^* p_\alpha p'_\beta - i \{ f(q^2) \varepsilon_\mu^* \\ + (\varepsilon^* \cdot p) [a_+(q^2) (p_\mu + p'_\mu) + a_-(q^2) (p_\mu - p'_\mu)] \}, \end{aligned} \quad (11)$$

$$\begin{aligned} \langle H_{0+}(p') | A_\mu | H_{0-}(p) \rangle \\ = F_+(q^2) (p_\mu + p'_\mu) + F_-(q^2) (p_\mu - p'_\mu), \end{aligned} \quad (12)$$

$$\begin{aligned} \langle H^{3P_1}(p', \varepsilon) | V_\mu - A_\mu | H_{0-}(p) \rangle \\ = -i \{ F'(q^2) \varepsilon_\mu^* + (\varepsilon^* \cdot p) [A'_+(q^2) (p_\mu + p'_\mu) \\ + A'_-(q^2) (p_\mu - p'_\mu)] \} + 2G'(q^2) \epsilon^{\mu\nu\alpha\beta} \varepsilon_\nu^* p_\alpha p'_\beta, \end{aligned} \quad (13)$$

$$\begin{aligned} \langle H^{1P_1}(p', \varepsilon) | V_\mu - A_\mu | H_{0-}(p) \rangle \\ = -i \{ F(q^2) \varepsilon_\mu^* + (\varepsilon^* \cdot p) [A_+(q^2) (p_\mu + p'_\mu) \\ + A_-(q^2) (p_\mu - p'_\mu)] \} + 2G(q^2) \epsilon^{\mu\nu\alpha\beta} \varepsilon_\nu^* p_\alpha p'_\beta. \end{aligned} \quad (14)$$

The calculation of the form factors in (10) and (11) for the case of  $B \rightarrow D(D^*)$  transitions has been done in [37]. However, for the sake of utility, the analytical expressions are reported in Appendix A. One of the main results of this paper is the calculation of the form factors appearing in (12)–(14). By way of an example, in the following we describe the calculation of the matrix element  $\langle H_{0+}(p') | A_\mu | H_{0-}(p) \rangle$  and give the expressions of the form factors  $F_\pm$ . In Appendix B we collect the expressions for  $G^{(\prime)}$ ,  $F^{(\prime)}$  and  $A_\pm^{(\prime)}$ . Note that all the calculations are done in the frame where  $q_3^\mu = (E_3, \mathbf{k} - \mathbf{q})$ ,  $q_1^\mu = (E_1, \mathbf{k})$ ,  $q_2^\mu = (E_2, -\mathbf{k})$ .

Let us start considering the  $0^- \rightarrow 0^+$  transition,

$$\begin{aligned} \langle H_{0+}(p') | \bar{Q}_3 \gamma_\mu \gamma_5 Q_1 | H_{0-}(p) \rangle \\ = - \int_D \frac{d^3 k}{(2\pi)^3} \psi_{0+}^*(k) \psi_{0-}(k) \sqrt{\frac{m_1 m_3}{E_1 E_3}} \\ \times \text{Tr} \left[ \frac{-q_2 + m_2}{2m_2} (\gamma_0 \Gamma_{0+}(q_3, q_2)^\dagger \gamma_0) \frac{q_3 + m_3}{2m_3} \gamma_\mu \right. \\ \left. \times \gamma_5 \frac{q_1 + m_1}{2m_1} (\Gamma_{0-}) \frac{-q_2 + m_2}{2m_2} \right], \end{aligned} \quad (15)$$

<sup>1</sup> We do not consider in this paper the tensor mesons.

where  $\mathcal{D}$  is the integration domain [35–37] defined by

$$\begin{aligned} \max(0, k_-) &\leq k_- \leq \min(K_M, k_+), \\ \max(-1, f(k, |\mathbf{q}|)) &\leq \cos(\theta) \leq 1, \\ 0 &\leq \varphi \leq 2\pi, \end{aligned} \quad (16)$$

with

$$k_{\pm} = \frac{|\mathbf{q}| (m_F^2 + m_2^2) \pm (m_F^2 - m_2^2) \sqrt{m_F^2 + \mathbf{q}^2}}{2m_F^2}, \quad (17)$$

$$f(k, |\mathbf{q}|) = \frac{2\sqrt{m_F^2 + \mathbf{q}^2} \sqrt{k^2 + m_2^2} - (m_F^2 + m_2^2)}{2k|\mathbf{q}|}. \quad (18)$$

$\varphi$  and  $\theta$  are the azimuthal and the polar angles respectively for the 3-momentum  $\mathbf{k}$ .  $K_M = (m_1^2 - m_2^2)/(2m_1)$  and  $m_I$  ( $m_F$ ) is the mass of the initial (final) meson: in (15)  $m_F = m_{0+}$ . We choose the  $z$ -axis along the direction of  $\mathbf{q}$ , the (3-) momentum of the  $W$  boson (cf. Fig. 1).

The analytical expressions for the form factors can be obtained by comparing (15) with (12):

$$\begin{aligned} F_+(q^2) &= \int \frac{k^2 dk d \cos \theta \psi_I(k) \psi_F^*(k)}{8\pi^2 m_I \sqrt{(-d_{12}^2 + m_I^2)} (m_F^2 - s_{23}^2) E_1 E_3} \\ &\times \left[ d_{12} s_{23} E_2 - m_I ((d_{13} - 2m_2) m_2 + m_I E_2) \right. \\ &+ \frac{k}{|\mathbf{q}|} \cos(\theta) (-m_F^2 m_I + d_{12} s_{23} (m_I - E_F) \\ &\left. + m_I^2 E_F) \right], \end{aligned} \quad (19)$$

$$\begin{aligned} F_-(q^2) &= \int \frac{k^2 dk d \cos \theta \psi_I(k) \psi_F^*(k)}{8\pi^2 m_I \sqrt{(-d_{12}^2 + m_I^2)} (m_F^2 - s_{23}^2) E_1 E_3} \\ &\times \left[ m_2 m_I s_{13} + (m_I^2 + d_{12} s_{23}) E_2 \right. \end{aligned}$$

$$\begin{aligned} &- \frac{k}{|\mathbf{q}|} \cos(\theta) (m_F^2 m_I + d_{12} s_{23} (m_I + E_F) \\ &+ m_I^2 E_F) \end{aligned} \Big], \quad (20)$$

where ( $d_{ij} = m_i - m_j$  and  $s_{ij} = m_i + m_j$ ). The expressions for the remaining form factors in (10)–(14) are collected in Appendices A and B.

## 4 Fixing the free parameters

The numerical evaluation of the form factors given in Sect. 3 requires one to specify the expression for the vertex functions and the values of the free parameters of the model. For the vertex functions we adopt two possible forms, the gaussian-type, extensively used in literature (see for example [38–42]):

$$\psi_H(k) = 4\sqrt{M_H} \sqrt{\frac{\sqrt{\pi^3}}{\omega_H^3}} \exp \left\{ -\frac{k^2}{2\omega_H^2} \right\}, \quad (21)$$

and the exponential one:

$$\psi_H(k) = 4\pi \sqrt{\frac{M_H}{\omega_H^3}} \exp \left\{ -\frac{k}{\omega_H} \right\}, \quad (22)$$

which is able to fit the results of a relativistic quark model regarding the shape of the meson wave functions [43, 44]. In our approach  $\omega_H$  is a free parameter which should be fixed by comparing a set of experimental data with the predictions of the model. In this paper we choose to fix the free parameters by a fit to the experimental data on  $\text{Br}(B \rightarrow D \ell \nu)$  [45] and on the spectrum of the  $B \rightarrow D^* \ell \nu$  process [46, 47].

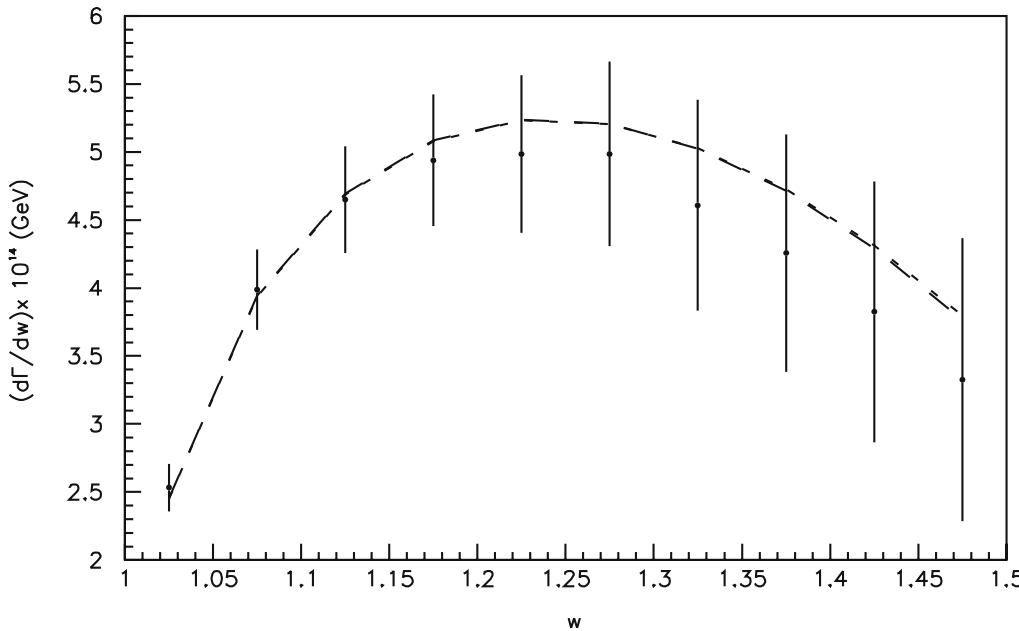


**Fig. 2.** The  $B \rightarrow D^* \ell \nu_\ell$  spectrum. The dashed (dotted) line corresponds to the exponential (Gaussian) vertex function. The data are taken from [46, 47]

The quality of the agreement between fitted spectrum and the corresponding experimental data may be assessed by looking at Fig. 2. It should be also observed that there are very small differences between the  $B \rightarrow D^* \ell \nu$  spectrum using the vertex functions in (21) and (22). Regarding the  $B \rightarrow D \ell \nu$  branching ratio, we obtain  $2.00(2.01)\%$  for the exponential (Gaussian) vertex function to be compared to the experimental value:  $\text{Br}(B \rightarrow D \ell \nu) = 2.15 \pm 0.22(2.12 \pm 0.20)\%$  for the charged (neutral)  $B$  meson. At this stage the two different forms of the vertex functions agree equally well with the experimental data. However, differences emerge when single form factors are considered (cf. for example Table 3).

## 5 Heavy quark limit

In this section we perform the heavy quark limit for the form factors obtained in the previous sections. Before we do this we briefly recall the implications of the HQET on the heavy meson spectrum. In the quark model, mesons are conventionally classified according to the eigenvalues of the observables  $J$ ,  $L$  and  $S$ : any state is labelled with the symbol  ${}^{2S+1}L_J$ . So, if we consider the lower-lying even parity mesons ( $L=1$ ), the scalar and the tensor mesons correspond to the  ${}^3P_0$  and  ${}^3P_2$  states, respectively. Moreover, there are two states with  $J=1$ :  ${}^1P_1$  and  ${}^3P_1$ , and they can mix if the constituent quark masses are different as in the case of charmed mesons. For heavy mesons the decoupling of the spin of the constituent heavy quark,  $s_Q$ , suggests one to use a different set of observables: the total angular momentum of the light constituent,  $j_q (= s_q + L)$ , the orbital momentum of the light degrees of freedom with respect to the heavy quark,  $L$ , the total angular momentum  $J (= j_q + s_Q)$ , and any state is labelled with  $L_J^{j_q}$ . In this representation the scalar and the tensor mesons are labelled by  $P_0^{1/2}$  and  $P_2^{3/2}$ , respectively. The axial mesons are classified as  $P_1^{3/2}$  and  $P_1^{1/2}$  and are related to the  ${}^3P_1$  and  ${}^1P_1$  states by [24]

$$\left| P_1^{3/2} \right\rangle = \sqrt{\frac{2}{3}} \left| {}^1P_1 \right\rangle + \sqrt{\frac{1}{3}} \left| {}^3P_1 \right\rangle, \quad (23)$$

$$\left| P_1^{1/2} \right\rangle = \sqrt{\frac{1}{3}} \left| {}^1P_1 \right\rangle - \sqrt{\frac{2}{3}} \left| {}^3P_1 \right\rangle. \quad (24)$$

The scaling laws of the HQET concern the  $0^- \rightarrow (P_0^{1/2}, P_1^{1/2}, P_1^{3/2})$  form factors; they are defined combining the form factors in (12)–(14) and the relations in (23) and (24). For example  $G^{1/2}(q^2) \equiv \sqrt{1/3}G(q^2) - \sqrt{2/3}G'(q^2)$ .

To extract the heavy quark mass dependence from the expressions of the form factors we follow the same approach as used in our previous paper [37]. We introduce the variable  $x$ , defined by  $x = (2\alpha k)/m_F$ , and in such a way, neglecting the light quark mass with respect to the heavy ones, the integration domain, near the zero-recoil point, will simplify to  $0 \leq x \leq \alpha$ ,  $0 \leq \theta \leq \pi$  and  $0 \leq \varphi \leq 2\pi$ . Therefore, if we look at the expressions of  $F_{\pm}(q^2)$ , (19)–(20), near

the zero-recoil point (i.e.  $q^2 \simeq q_{\max}^2$ ) we have, neglecting terms of the order of  $x^3$ ,

$$F_{\pm}(q^2)|_{q^2 \simeq q_{\max}^2} = \int_0^\alpha dx \psi_I(k(x)) \psi_F(k(x)) \times \frac{m_F^2 (m_F \mp m_I) (7 - 3w) x^2}{384 m_I \pi^2 \alpha^3}. \quad (25)$$

For  $\alpha \ll 1$  the integration can easily be done, giving

$$F_{\pm}(q^2)|_{q^2 \simeq q_{\max}^2} = \frac{m_F \mp m_I}{\sqrt{m_F m_I}} \times \begin{cases} \left[ 2\sqrt{2} \left( \frac{\omega_I \omega_F}{\omega_I^2 + \omega_F^2} \right)^{3/2} \right] \frac{1}{3} \left( 1 - \frac{3}{4}(w-1) \right) + o((w-1)^2) & \text{Gaussian-type} \\ \left[ 8 \frac{\sqrt{\omega_I^3 \omega_F^3}}{(\omega_I + \omega_F)^3} \right] \frac{1}{3} \left( 1 - \frac{3}{4}(w-1) \right) + o((w-1)^2) & \text{exponential-type.} \end{cases} \quad (26)$$

Thus, the  $\tau_{1/2}$  Isgur–Wise function resulting from our model is given by

$$\tau_{1/2}(w) = \frac{1}{3} - \frac{1}{4}(w-1) + \frac{19}{96}(w-1)^2 + o((w-1)^3), \quad (27)$$

where we have also written the term  $(w-1)^2$  which was neglected in (26).

A similar analysis can be performed on the heavy to heavy  $0^- \rightarrow P_1^{1/2}$  form factors. Let us start considering the combination

$$\left\{ \begin{array}{l} G^{1/2}(q^2) \\ F^{1/2}(q^2) \\ A_{\pm}^{1/2}(q^2) \end{array} \right\} = \frac{1}{\sqrt{3}} \left\{ \begin{array}{l} G(q^2) \\ F(q^2) \\ A_{\pm}(q^2) \end{array} \right\} - \sqrt{\frac{2}{3}} \left\{ \begin{array}{l} G'(q^2) \\ F'(q^2) \\ A'_{\pm}(q^2) \end{array} \right\}, \quad (28)$$

which defines the  $0^- \rightarrow P_1^{1/2}$  form factors. It is very simple to obtain their scaling laws in the limit of heavy quark masses. Following the above method we obtain

$$\left\{ \begin{array}{l} G^{1/2}(q^2) \\ F^{1/2}(q^2) \\ A_{\pm}^{1/2}(q^2) \end{array} \right\} = N \left\{ \begin{array}{l} \sqrt{m_I m_F} \\ \mp 1/\sqrt{m_I m_F} \\ (w-1) \end{array} \right\} \frac{1}{3} \left( 1 - \frac{3}{4}(w-1) \right) + o((w-1)^2), \quad (29)$$

where

$$N = \begin{cases} 2\sqrt{2} \left( \frac{\omega_I \omega_F}{\omega_I^2 + \omega_F^2} \right)^{3/2} & \text{Gaussian-type} \\ 8 \frac{\sqrt{\omega_I^3 \omega_F^3}}{(\omega_I + \omega_F)^3} & \text{exponential-type} \end{cases}. \quad (30)$$

Similarly, we can evaluate the  $\tau_{3/2}$  Isgur–Wise function obtaining

$$\tau_{3/2}(w) = \frac{5}{6} - \frac{31}{24}(w-1) + \frac{93}{64}(w-1)^2 + o((w-1)^3). \quad (31)$$

**Table 1.** The two best fit sets of values of the free parameters are obtained for the exponential (exp.) and Gaussian (Gauss.) vertex function

Parameter	fitted values (exp.)	fitted values (Gauss.)
$m_q$	23 MeV	34 MeV
$\omega_B$	101 MeV	108 MeV
$\omega_D = \omega_{D^*} = \omega_{D^{**}}$	51 MeV	186 MeV
$ V_{cb} $	0.041	0.043

**Table 2.** The Isgur–Wise functions  $\tau_{1/2}$  and  $\tau_{3/2}$  at zero recoil and their slope parameters

$\tau_{1/2}(1)$	$\varrho_{1/2}^2$	$\tau_{3/2}(1)$	$\varrho_{3/2}^2$	Ref.
0.33	0.75	0.83	1.29	This work
0.34	0.76	0.59	1.09	[11, 12]
0.22	0.83	0.54	1.5	[48]
0.31	1.18	0.61	1.73	[49]
$0.13 \pm 0.04$	$0.50 \pm 0.05$	$0.43 \pm 0.09$	$0.90 \pm 0.05$	QCDSR [53]
$0.35 \pm 0.08$	$2.5 \pm 1.0$	—	—	QCDSR(NLO) [52]
$0.38 \pm 0.04$		$0.53 \pm 0.08$		Lattice [50]

A comparison between our results and some others, coming from quark models, QCD sum rules and lattice calculations, can be done looking at the Table 2. The values of the  $\tau$  functions at zero-recoil point and their slopes are compatible. In particular, it should be observed that our results for  $\tau_{1/2}$  are practically the same as obtained in the Isgur–Scora–Grinstein–Wise (ISGW) model [11, 12] and QCD sum rules findings [52, 53].<sup>2</sup> Regarding  $\tau_{3/2}$ , our result at the zero-recoil point is slightly larger than the results coming from other models, while the slope is comparable with the other ones.

Relations between the slope of the Isgur–Wise function and  $\tau$  functions at zero-recoil points were derived, in the form of sum rules, by Bjorken [54] and Uraltsev [55]:

$$\varrho^2 - \frac{1}{4} = \sum_n |\tau_{1/2}^{(n)}(1)|^2 + 2 \sum_n |\tau_{3/2}^{(n)}(1)|^2, \quad (32)$$

$$\frac{1}{4} = \sum_n |\tau_{3/2}^{(n)}(1)|^2 - \sum_n |\tau_{1/2}^{(n)}(1)|^2, \quad (33)$$

where  $n$  stands for the radial excitations and  $\varrho^2$  is the slope of the Isgur–Wise function  $\xi(w)$ , which in our model [37] is

$$\xi(w) = 1 - \frac{11}{12}(w-1) + \frac{77}{96}(w-1)^2 + o((w-1)^3). \quad (34)$$

Our results for  $n=0$  oversaturate both the sum rules. For the Bjorken sum rule this is due to the small value we obtain for the derivative of the Isgur–Wise function ( $\varrho^2$ ) which is in any case compatible with the experimental value  $\varrho^2 = 0.95 \pm 0.09$  [46, 47]. We plan to study this problem in a separate work. However, a detailed discussion of

these sum rules and the findings of quark models can be found in [56].

## 6 Numerical results and discussion

All the results discussed in the previous section have been obtained without fixing the free parameters of the model. In this one we use the fitted values of the free parameters in Table 1 (cf. Sect. 4 for discussion) to obtain the numerical results of the form factors. First of all, in Table 3 are collected the values of the form factors for the  $B \rightarrow D^{**}$  transitions evaluated at zero-recoil point ( $q_{\max}^2 = (m_B - m_{D^{**}})^2$ ) and at  $q^2 = 0$ . We consider the charmed final state with the following masses:  $m(D_0^*) = 2.40$  GeV,  $m(D'_1) = 2.43$  GeV,  $m(D_1) = 2.42$  GeV [45].<sup>3</sup> Note that we are considering, for a better comparison with other calculations, the helicity form factors (cf. for definitions, for example, [58]). Looking at Table 3, we can see that the absolute values of our form factors (at  $q^2 = 0$ ) are larger than the ones in [11, 12, 26], this naturally implies larger branching ratios in our model. In particular, our predictions on the branching ratios, using the exponential (Gaussian) vertex function, are ( $\tau_{B^0} = 1.536 \times 10^{-12}$  s [45])

$$\begin{aligned} \text{Br}(\bar{B}^0 \rightarrow D_0^{*+} \ell^- \bar{\nu}_\ell) &= 2.3(2.1) \times 10^{-3} (|V_{cb}|/0.041)^2, \\ \text{Br}(\bar{B}^0 \rightarrow D'_1{}^+ \ell^- \bar{\nu}_\ell) &= 2.0(1.6) \times 10^{-3} (|V_{cb}|/0.041)^2, \\ \text{Br}(\bar{B}^0 \rightarrow D_1^+ \ell^- \bar{\nu}_\ell) &= 8.0(7.3) \times 10^{-3} (|V_{cb}|/0.041)^2. \end{aligned} \quad (35)$$

<sup>2</sup> The values and the slopes of  $\tau$  functions are obtained fitting the numerical results obtained in Morenas et al. [13–19] using the ISGW model.

<sup>3</sup>  $D'_1$  and  $D_1$  represent, respectively, the two different physical axial-vector charmed meson states. The physical  $D'_1$  ( $D_1$ ) is primarily  $P_1^{1/2}$  ( $P_1^{3/2}$ ). They differ by a small amount from the mass eigenstates in the heavy quark limit; for a discussion see [57]. In this paper we neglect these differences.

**Table 3.**  $B \rightarrow D^{**}$  form factors evaluated at  $q^2 = 0$  and at  $q_{\max}^2 = (m_B - m_{D^{**}})^2$  by using the vertex function in (22). In parentheses the values obtained using the Gaussian vertex function (cf. (21))

Form factor	This work		[11, 12]		[26]	
	$F(0)$	$F(q_{\max}^2)$	$F(0)$	$F(q_{\max}^2)$	$F(0)$	$F(q_{\max}^2)$
$F_1$	-0.32 (-0.30)	-0.35 (-0.33)	-0.18	-0.24	-0.24	-0.34
$F_0$	-0.32 (-0.30)	-0.025 (-0.036)	-0.18	0.008	-0.24	-0.20
$A_0^{(1/2)}$	-0.25 (-0.23)	-0.31 (-0.28)	-0.18	-0.39	-0.075	-0.083
$A_1^{(1/2)}$	0.096 (0.088)	-0.0018 (-0.0029)	0.070	-0.002	0.073	0.071
$A_2^{(1/2)}$	0.69 (0.63)	0.87 (0.79)	0.49	0.91	0.32	0.56
$V^{(1/2)}$	0.67 (0.61)	0.84 (0.76)	0.44	0.81	0.31	0.55
$A_0^{(3/2)}$	-0.61 (-0.58)	-0.81 (-0.77)	-0.20	-0.46	-0.47	-0.76
$A_1^{(3/2)}$	-0.13 (-0.13)	-0.016 (-0.023)	-0.005	-0.008	-0.20	-0.26
$A_2^{(3/2)}$	0.70 (0.65)	1.27 (1.19)	0.33	0.72	0.25	0.47
$V^{(3/2)}$	-0.81 (-0.77)	-1.09 (-1.03)	-0.44	-0.71	-0.61	-1.24

**Table 4.** Parameters of the  $B \rightarrow D^{**}$  form factors. The functional  $q^2$  dependence is either polar :  $F(q^2) = F(0)/(1 - aq^2/m_B^2)$  or linear:  $F(q^2) = F(0)(1 + bq^2)$ . In parentheses the values obtained using the Gaussian vertex function (cf. (21))

Form factor	$F(0)$	$a$	$b (\text{GeV}^{-2})$
$F_1$	-0.32 (-0.30)	0.263 (0.233)	
$F_0$	-0.32 (-0.30)		-0.109 (-0.103)
$A_0^{(1/2)}$	-0.25 (-0.23)	0.661 (0.626)	
$A_1^{(1/2)}$	0.10 (0.092)		-0.120 (-0.120)
$A_2^{(1/2)}$	0.69 (0.64)	0.695 (0.680)	
$V^{(1/2)}$	0.67 (0.61)	0.695 (0.679)	
$A_0^{(3/2)}$	-0.61 (-0.59)	0.846 (0.834)	
$A_1^{(3/2)}$	-0.13 (-0.13)		-0.102 (-0.0956)
$A_2^{(3/2)}$	0.72 (0.67)	1.53 (1.54)	
$V^{(3/2)}$	-0.81 (-0.77)	0.872 (0.873)	

Regarding the  $q^2$  dependance of the form factors, we find a very good agreement with numerical results assuming the following polar expression:

$$F(q^2) = \frac{F(0)}{1 - a \frac{q^2}{m_B^2}}, \quad (36)$$

the fitted values of  $a$  can be found in Table 4. It is interesting to observe that the effective pole mass is not far from the mass of the  $B_c$  meson. A different  $q^2$  dependence exhibit the form factors  $F_0$  and  $A_1$ ; for them we use the form

$$F(q^2) = F(0)(1 + bq^2), \quad (37)$$

and the values of  $b$  are collected in Table 4.

In conclusion we have obtained in a very simple constituent quark model all the semileptonic form factors relevant to the transition of  $B$  into the low-lying odd and even parity charmed mesons. The free parameters of the model

have been fixed by comparing model predictions with the  $B \rightarrow D^* \ell \nu$  spectrum and  $B \rightarrow D \ell \nu$  branching ratio. Our numerical results are generally larger than the results of other models. However, form factors reproduce the scaling laws dictated by the HQET in the limit of infinitely heavy quark masses.

## Appendix A: Form factors $f_{\pm}$ , $g$ , $f$ , $a_{\pm}$

In this appendix we collect the analytical expressions for the  $0^- \rightarrow 0^-$  and  $0^- \rightarrow 1^-$  form factors defined in (10) and (11), respectively. We have

$$f_+(q^2) = \int k^2 dk d \cos \theta \times \frac{\psi_I(k) \psi_F^*(k)}{8\pi^2 m_I \sqrt{(d_{23}^2 - m_F^2) (d_{12}^2 - m_I^2) E_1 E_3 (m_F^2 - E_F^2)}}$$





37. M. De Vito, P. Santorelli, Eur. Phys. J. C **40**, 193 (2005) [hep-ph/0412388]
38. M.A. Ivanov, P. Santorelli, Phys. Lett. B **456**, 248 (1999) [hep-ph/9903446]
39. M.A. Ivanov, J.G. Korner, P. Santorelli, Phys. Rev. D **63**, 074010 (2001) [hep-ph/0007169]
40. M.A. Ivanov, J.G. Korner, P. Santorelli, Phys. Rev. D **70**, 014005 (2004) [hep-ph/0311300]
41. M.A. Ivanov, J.G. Korner, P. Santorelli, Phys. Rev. D **71**, 094006 (2005) [hep-ph/0501051]
42. M.A. Ivanov, J.G. Korner, P. Santorelli, Phys. Rev. D **73**, 054024 (2006) [hep-ph/0602050]
43. P. Cea, P. Colangelo, L. Cosmai, G. Nardulli, Phys. Lett. B **206**, 691 (1988)
44. P. Colangelo, G. Nardulli, M. Pietroni, Phys. Rev. D **43**, 3002 (1991)
45. Particle Data Group, S. Eidelman et al., Phys. Lett. B **592**, 1 (2004)
46. CLEO Collaboration, R.A. Briere et al., Phys. Rev. Lett. **89**, 081803 (2002) [hep-ex/0203032]
47. BABAR Collaboration, B. Aubert, hep-ex/0408027
48. V. Morenas, A. Le Yaouanc, L. Oliver, O. Pene, J.C. Raynal, Phys. Rev. D **56**, 5668 (1997) [hep-ph/9706265]
49. H.Y. Cheng, C.K. Chua, C.W. Hwang, Phys. Rev. D **69**, 074025 (2004) [hep-ph/0310359]
50. D. Becirevic et al., Phys. Lett. B **609**, 298 (2005) [hep-lat/0406031]
51. A. Deandrea, N. Di Bartolomeo, R. Gatto, G. Nardulli, A.D. Polosa, Phys. Rev. D **58**, 034004 (1998) [hep-ph/9802308]
52. P. Colangelo, F. De Fazio, N. Paver, Phys. Rev. D **58**, 116005 (1998) [hep-ph/9804377]
53. Y.B. Dai, M.Q. Huang, Phys. Rev. D **59**, 034018 (1999) [hep-ph/9807461]
54. J.D. Bjorken, SLAC-PUB-5278, Invited talk given at Les Rencontres de la Valle d'Aoste, La Thuile, Italy, March 18–24, 1990
55. N. Uraltsev, Phys. Lett. B **501**, 86 (2001) [hep-ph/0011124]
56. I.I. Bigi et al., hep-ph/0512270
57. H.Y. Cheng, C.K. Chua, hep-ph/0605073
58. F. Buccella, M. Lusignoli, G. Miele, A. Pugliese, P. Santorelli, Phys. Rev. D **51**, 3478 (1995) [hep-ph/9411286]